Kinematic Design of a Configurable Terrain Simulator Platform for Robotic Legs

Yifu Gao, Victor Barasuol, Darwin G. Caldwell and Claudio Semini
All authors are with the Department of Advanced Robotics, Istituto Italiano di Tecnologia (IIT), 16163 Genova, Italy
E-mail: firstname.lastname@iit.it

Abstract: This paper presents the design of a novel configurable Terrain Simulator Platform (TSP) developed for robotic legs to test and verify their motion performance during the interaction with different terrains. The TSP is a test device able to emulate different terrains such as slope, vertical step, stairs and even dynamically varied terrain by the movements of the moving platform to simulate complicated terrains in natural environments. A planar $\underline{P}$RR parallel mechanism is chosen to produce desired motions of the moving platform. The kinematics of the $\underline{P}$RR mechanism including forward and inverse kinematics are presented. Different types of singularities are studied and analysed. The measures adopted in design to get rid of forward kinematics singularity in desired workspace are presented. At last, the workspace without forward singularity are obtained.

Key Words: Terrain Simulator Platform, Robotic Leg, $\underline{P}$RR Planar Parallel Mechanism, Workspace Singularity

1 INTRODUCTION

Legged robots have been supposed as a promising solution to rough terrain on earth for a long time, where traditional wheeled or tracked vehicles could not traverse effectively [1]. During recent decades diverse types of legged robots are developed including humanoid robots with two legs [2], mammal-like quadruped robots [3, 4, 5] and insect-like multi-legged robots [6, 7].

By reviewing previous works it is notable that the design and control of robotic legs often play an important role in the development of robots. Robot legs will not only determine to a great extent the mobility of robots such as the locomotion velocity and the capability of overcoming obstacles but also influence the integrated performance of the entire robotic system, i.e. payload capacity, energy consumption, versatility — motions able to be realized by robot, etc. The majority of robotic legs are often designed for specified robotic system and can be fully tested only after the construction of the entire robot. This will considerably confine the application range of specifically developed robotic legs, indeed robotic legs are seldom to be transplanted to other platforms besides its original system, and make the development of legged robots complicated and time-consuming. If the design and control of robotic legs can be tested and validated independently rather than under the frame of the entire robotic system, it is possible to refine and improve the design of legs and furthermore optimize the performance of the robot. Moreover based on the acquired knowledge on robotic legs, robots with the same leg design but different body size, shape and number of legs could also be developed conveniently for diverse applications.

Test benches developed for single legged robot or robotic leg experiments can be traced back to Marc Raibert's tether mechanism used in the research of planar one-legged hopping machine [8]. A similar mechanism is also adopted in [9]. However, these mechanisms can barely provide single leg robots a constrained surrounding for basic motion tests. Apart from tether mechanisms, instrumented treadmills are another widely-used facilities to execute the locomotion and gait research experiments for humans, animals and legged robots. Instrumented treadmills are often equipped with force sensors or force plates under the track to measure the ground reaction forces. Additionally, some special instrumented treadmills have lifting mechanism to change the gradient of the track. The advantages of instrumented treadmills is analysed in [10]. But there are also some limitations for instrumented treadmills to conduct experiments simulating the actual foot-terrain interaction that occurs in natural environment, e.g.: 1) the mechanical properties of ground/contact surface, i.e. stiffness, coefficient of friction and viscosity etc., in natural environment are diverse. However the material of surface layer of a treadmill is usually unchanged; 2) although few instrumented treadmills have movable tracks, the range and speed of track motion are rather limited due to the size and the weight of the track. Therefore, common instrumented treadmills lack the function of dynamically adjusting the track gradient and height to simulate the fast and complex terrain variation experienced by robots in rough-environment locomotion such as running on rocky terrain or climbing stairs.

In this paper, we present the design of the configurable Terrain Simulator Platform (TSP), which is able to provide specified foothold positions and orientations for robotic legs by the movements of either a pedal or a small treadmill as the moving platform, to simulate diverse gaits on complex terrain. Figure 1 shows the structure of TSP with pedal configuration.

The next sections of this paper are organized as follows.

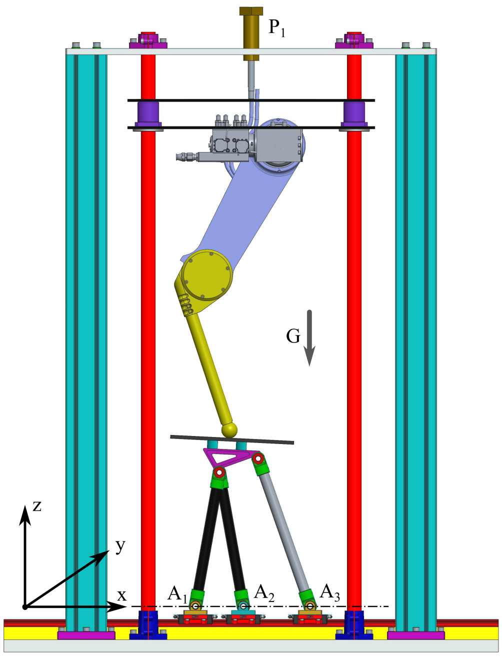

Figure 1: TSP structure in pedal configuration. TSP has 4 actuated prismatic joints, one connects the frame/base and the hip fixture to adjust the vertical position of leg (joint P_1); the other three are arranged in the bottom of the base to actuate three sliders moving along x-direction (sliders A_1, A_2 and A_3). The three hydraulic actuators in the bottom of the base construct a parallel mechanism in vertical plane, a pedal is adopted as end-effector to simulate the desired rough terrain to interacting with the foot of the leg.

Section 2 analyses some characteristic motions of robotic legs and the design specification of the TSP is proposed based on these characteristic motions. In Section 3, the structure of the TSP is presented and its forward and inverse kinematics are derived. Singularities features and workspace of the $\underline{P}$RR planar parallel mechanism adopted are studied in Section 4. The measures taken to solve the influence caused by singularities are provided as well. The aspect of workspace of this mechanism without singularity is obtained and presented. At last, conclusions are presented.

2 TSP Design Specifications Based on Robot Characteristic Motions

In order to determine the TSP specifications, the characteristic motions of robotic legs are analysed and studied beforehand. Usually the legs of diverse types of robots have varied structure, for example the legs of humanoid robots often consist of 6 DoF (Degree of Freedom) for each leg. Quadruped or six-legged robot legs typically include 3 to 4 active DoFs [4][6][11][12][13]. Although structures of legs may differ, the behaviours of legs in the plane of motion defined by the forward velocity vector and gravity vector are essentially similar. And moreover the motions in this plane contribute most of power to the progression of robot [8]. Via comparing the mobility including locomotion velocity, payload capability, rough terrain suitability of different types of robots built in comparable size and mass, it is notable that hydraulically actuated quadruped robots featured with dynamic balance and gaits such as BigDog and HyQ possess superior mobility of all. Therefore we take the leg parameters and characteristic motions of the hydraulically actuated quadruped robot HyQ2Max [3] as research subject to draw up design specification of the TSP, thus the TSP will accommodate a larger variety of robotic legs.

Among all parameters of some gaits, what we care most for the design of the TSP are the ground reaction forces (GRF) caused by the characteristic motions. Since these parameters will determine the motions and payload of the TSP directly. In reference [3] some characteristic motions have already been simulated and presented, in this paper additional dynamic motions including flying trot at velocity up to $2.75m/s$ and jump are taken into consideration to find out the extreme motion parameters. From these motion simulations, corresponding ground reaction forces acting on the feet of robot weighing 120 kg are acquired. The data of the GRFs of the right hind (RH) leg, shown in Fig. 2, are taken as example. The other legs GRFs are similar to that from the RH leg with less than 15% difference.

Based on Fig. 2 the payload specification of the TSP can be determined. Combining with kinematic parameters of robotic leg and gait, the motion parameters including motion range and motion velocity are proposed in Table 1.

Table 1: Design Specification

horizontal motion range	$0.5m$
horizontal motion velocity	$-2.75 \sim 2.75m/s$
horizontal payload (Max.)	$\pm 500N$
vertical motion range	$0.2m$
vertical motion velocity	$-2.5 \sim 2.5m/s$
vertical payload (continuous)	$1000N$
rotation range about y-axis	$\pm 45^\circ$, pedal configuration
rotation range about y-axis	$\pm 14^\circ$, treadmill configuration
angular velocity about y-axis	$900^\circ/s$

3 Design of the TSP

The TSP consists of 4 DoFs for the pedal configuration, shown in Fig. 1, or 5 DoFs for treadmill configuration (in which the pedal is replaced by a light-weight treadmill, shown in Fig. 3) .

One of the degree-of-freedom is the vertical linear motion of the hip fixture with respect to the base frame, which is used to change the height of hip joint of the leg. The other three DoFs form a $\underline{P}$RR mechanism in the vertical plane. A $\underline{P}$RR mechanism is comprised by 3 kinematic chains between the base and the moving platform [14]. Each chain embraces 3 joints in series from base: 1 prismatic joint and 2 revolute joints denoted by P and R respectively. The prismatic joints mounted on the base are actuated joints and represented as $\underline{P}$. The other revolute joints are passive. The moving platform of the $\underline{P}$RR mechanism is considered as end-effector to interact with the foot of the robotic leg. Thus the moving platform (part PQT in Fig. 4) can move in x and z directions linearly and rotate along y-axis in the xz plane. Compared with serial mechanisms with the same degree-of-freedom configuration, $\underline{P}$RR has

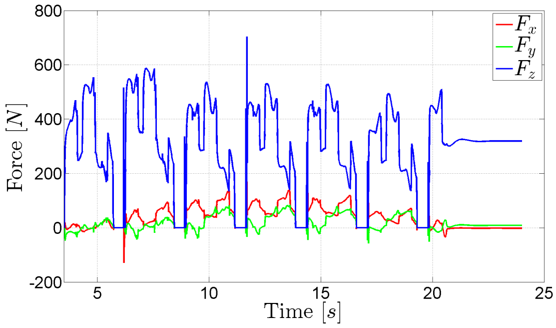

a) $0.12m$-high step climbing

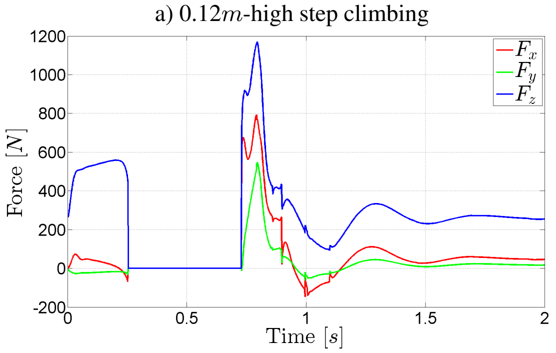

b) $0.3m$ high squat jump

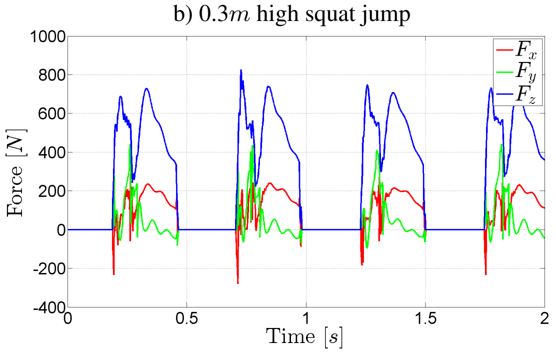

c) walking trot at $1.5m/s$ with step frequency $2Hz$

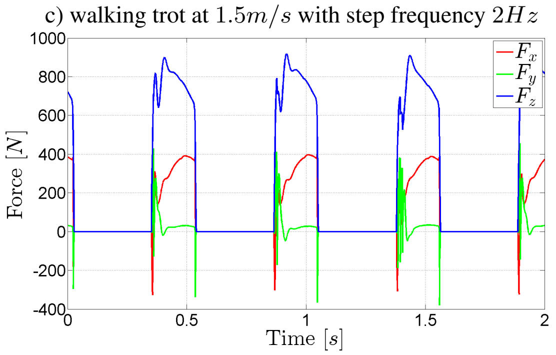

d) flying trot at $2.75m/s$ with step frequency $2Hz$

Figure 2: Ground reaction forces of 4 characteristic motions: a) $0.12m$-high step climbing, b) $0.3m$ high squat jump, c) walking trot at $1.5m/s$ with step frequency $2Hz$, d) flying trot at $2.75m/s$ with step frequency $2Hz$. The coordinate system corresponds to the definition adopted in [3], z-axis points up vertically, x-axis aligns with the forward locomoting direction. In total 120 kg of mass, including 40 kg payload on the torso, is set as mass parameter of the robot for the simulations.

advantages in the aspects of stiffness accuracy and payload capability but limitations in complexity of kinematics and confined workspace. Because most of the leg motions in forward progressing are periodic movements, we suppose that adopting a treadmill as moving platform instead of a pedal is helpful to reduce the inertial load caused by the repeatable movements of the moving platform. Thus the TSP will have a configurable structure for different application scenarios. When simulating the locomotion on rough terrain usually at a lower velocity such as walking on stairs or rocky terrain, the TSP works in the pedal configuration to produce steeper slope, more height difference in vertical direction and a quickly varying contact plane. On the controversy, for simulating locomotion on moderate rough/uneven terrain or fast locomotion such as flying trot progressing at $2.75m/s$, the TSP will be changed into the treadmill configuration mode to provide higher velocity relative to the hip or base frame.

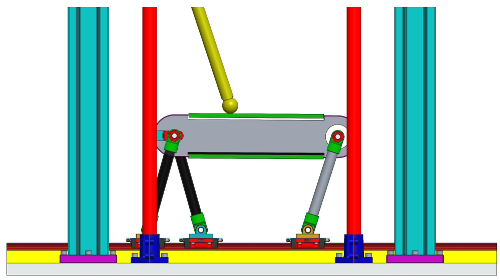

Figure 3: Structure of the TSP in treadmill configuration. A light-weight treadmill is designed to be the moving platform of PRR mechanism. The treadmill rotates in one single direction and its effective length (centre-to-centre distance of $0.6m$) can cover the entire step length of a trotting gait at 2 m/s with 2 Hz step frequency, and 0.5 duty factor (leg stance period over the step period).

3.1 Inverse Kinematics

The position and orientation of the moving platform PQT (see Fig. 4) in the base reference frame can be defined as $\mathbf{x}_{O'} = [x_{O'}, z_{O'}, \varphi]^T$. Once $\mathbf{x}_{O'}$ is given, the coordinate transformation of the points from the frame $O'x'y'z'$ to base frame can be expressed as:

$$\mathbf{r} = \begin{bmatrix} x_r \\ z_r \end{bmatrix} = \begin{bmatrix} x_{O'} \\ z_{O'} \end{bmatrix} + R(\varphi)\mathbf{r}_{O'} \tag{1}$$

$R(\varphi)$ is the rotation matrix along y-axis with angular magnitude φ, then

$$R(\varphi) = \begin{bmatrix} cos\varphi & sin\varphi \\ -sin\varphi & cos\varphi \end{bmatrix}$$

$\mathbf{r}$ and $\mathbf{r}_{O'}$ are the coordinate vectors of the same point expressed in the base frame and $O'x'y'z'$ reference frame separately. For pivots P and T, $\mathbf{r}_{O'}$ is constant and able to be written respectively as:

$$\overrightarrow{O'P} = [\frac{l_5}{2} - l_4 \cos\alpha, -l_4 \sin\alpha]^T$$

$$\overrightarrow{O'T} = [\frac{l_5}{2}, 0]^T$$

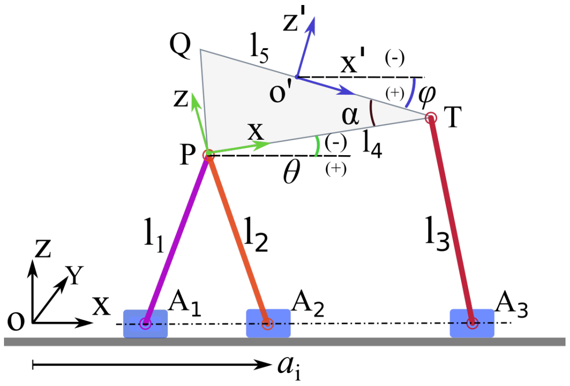

Figure 4: Schematic diagram of the TSP. $A_i(i=1,2,3)$ are sliders driven by linear actuators mounted in the base and only able to move in ox direction. The coordinate values of sliders $a_i(i=1,2,3)$ in base reference frame $Oxyz$ are selected as joint variables. A_1P, A_2P and A_3T are the links connecting the moving platform PQT to the sliders, their lengths are $l_i(i=1,2,3)$, respectively. The coordinate frame $O'x'y'z'$ fixed on moving platform PQT is set in the middle of the contact plane QT and has its x-axis aligned with QT. The geometric parameters of the moving platform PQT are defined as $l_i(i=4,5)$ and the angle α. A medium coordinate frame $Pxyz$ locates at the centre of pivot P and keeps its x-axis pointing to T . For treadmill configuration, $\alpha=0$ and $l_4=l_5$.

For given $\mathbf{x}_{O'}$, $[x_{O'}, z_{O'}]^T$ is known, then according to Eq. 1, $[x_P, z_P]^T$ and $[x_T, z_T]^T$ can be solved. Furthermore the joint variables $a_i(i=1,2,3)$ can be easily computed as:

$$a_i = x_P \pm \sqrt{l_i^2 - z_P^2} \qquad (i=1,2)$$

$$a_3 = x_T \pm \sqrt{l_3^2 - z_T^2}\ .$$

For general architecture of $\underline{\text{P}}$RR mechanism, there can be up to 8 inverse kinematics solutions in total. This may lead to complexity in the decision of joint variables. In order to reduce the number of redundant solutions, following additional geometric relationships below are taken in the design of the TSP,

$$l_1 = l_2$$

and

$$a_1 < a_2$$

then only two joint variable vectors

$$\mathbf{u} = [x_P - \sqrt{l_1^2 - z_P^2}, x_P + \sqrt{l_1^2 - z_P^2}, x_T \pm \sqrt{l_3^2 - z_T^2}]^T$$

will be obtained.

3.2 Forward Kinematics

For a given input vector $\mathbf{u} = [a_1, a_2, a_3]^T$ composed by three displacements of actuators, the position and orientation of the moving platform $\mathbf{x}_{O'} = [x_{O'}, z_{O'}, \varphi]^T$ are obtained as follows. The position of the moving platform $[x_{O'}, z_{O'}]$ can be derived from Eq. 2.

$$\overrightarrow{OO'} = \begin{bmatrix} x_{O'} \\ z_{O'} \end{bmatrix} = \mathbf{p} + R(\theta)\mathbf{O}'_P \qquad (2)$$

where $R(\theta)$ is the rotational matrix from the reference frame P to base frame $Oxyz$, thus

$$R(\theta) = \begin{bmatrix} cos\theta & sin\theta \\ -sin\theta & cos\theta \end{bmatrix}$$

$\mathbf{p}$ is the vector from the origin of the base frame O pointing at pivot P. $\mathbf{p}$ can be solved according to $a_i, (i=1,2)$ and $l_1(=l_2)$ directly and independently from a_3. Theoretically, $\mathbf{p}$ has two solutions mirrored with respect to x-axis, but considering practical situation that pivot P can only move above x-axis, thus only the solution with positive z_P is adopted.

$$\mathbf{p} = \begin{bmatrix} x_P \\ z_P \end{bmatrix} = \left[\frac{a_1+a_2}{2}, \sqrt{l_1^2 - (\frac{a_2-a_1}{2})^2}\right]^T$$

$$\mathbf{O}'_P = [l_4 - \frac{l_5 cos\alpha}{2}, \frac{l_5 sin\alpha}{2}]^T\ .$$

$\mathbf{O}'_P$ is the position vector of point O' with respect to the reference frame P. $\mathbf{O}'_P$ is only concerning with the constant geometric parameters of the moving platform PQT. Furthermore the orientation of the PQT, φ can be solved from

$$\varphi = \theta + \alpha\iota \qquad (3)$$

where θ is the orientation of the link PT and solved by

$$\theta = \frac{\pi}{2} - \beta \pm \arccos(\frac{l_3^2 - l_4^2 - (a_3 - x_P)^2 - z_P^2}{2l_4\sqrt{(a_3-x_P)^2 + z_P^2}})$$

$$\beta = \arctan\frac{a_3 - x_P}{z_P}\ .$$

The two possible solutions for θ correspond to the two possible assembly mode in which PT links are mirrored with respect to a fictional line connecting P and A_3. The plus symbol means that point T locates at the upper side of the line PA_3, and the minus symbol means the point T is positioned below the line PA_3.

4 The TSP Workspace and Singularity Postures

The workspace of the parallel mechanism is not only determined by the joint limits of every actuator but also affected by the singularity positions in its workspace. In general the total workspace of the parallel mechanism is divided into aspects by singularities. When mechanism moves close to singularity poses, the motion transmission or payload affording performance will deteriorate. Moreover, the singularities of parallel mechanism can come from different situations [15]. Due to the existence of singularity especially in forward kinematics, the kinematics of parallel mechanism is more complicated than that of mechanism with serial chain. To remove or avoid the forward kinematics singularity in the desired workspace is always a key point of parallel mechanism research [16]. By differentiating Eq.

2 and 3, the Jacobian matrix of TSP's mechanism can be obtained:

$$\mathbf{J} = \begin{bmatrix} \frac{1}{2} - \frac{M_2 M_6}{M_1} & \frac{1}{2} - \frac{M_2 M_7}{M_1} & \frac{M_2 M_4}{M_1} \\ -M_5 - \frac{M_3 M_6}{M_1} & M_5 - \frac{M_3 M_7}{M_1} & \frac{M_3 M_4}{M_1} \\ \frac{M_6}{M_1} & \frac{M_7}{M_1} & -\frac{M_4}{M_1} \end{bmatrix} \quad (4)$$

Where

$$M_1 = 2l_4(\frac{a_1 + a_2 - 2a_3}{2} sin\theta + cos\theta \sqrt{l_1^2 - (\frac{a_1 - a_2}{2})^2})$$

$$M_2 = \frac{2l_4 - l_5 cos\alpha}{2} sin\theta - \frac{l_5 sin\alpha}{2} cos\theta$$

$$M_3 = \frac{2l_4 - l_5 cos\alpha}{2} cos\theta + \frac{l_5 sin\alpha}{2} sin\theta$$

$$M_4 = a_1 + a_2 - 2a_3 + 2l_4 cos\theta$$

$$M_5 = \frac{a_1 - a_2}{4\sqrt{l_1^2 - (\frac{a_1 - a_2}{2})^2}}$$

$$M_6 = a_2 - a_3 + 2l_4(\frac{cos\theta}{2} + M_8)$$

$$M_7 = a_1 - a_3 + 2l_4(\frac{cos\theta}{2} - M_8)$$

$$M_8 = sin\theta \frac{a_1 - a_2}{4\sqrt{l_1^2 - (\frac{a_1 - a_2}{2})^2}} .$$

The conditions of singularities and corresponding postures of the mechanism can be obtained by studying the Jacobian matrix and its determinant. When

$$a_1 = a_2$$

and

$$a_3 = \frac{a_1 + a_2}{2} + l_4 cos\theta$$

occurs, $M_4 = 0, M_5 = 0, M_6 = M_7, M_8 = 0$, and the mechanism will be in the inverse kinematics singularities. In this pose the moving platform PQT cannot support the load in x direction. In order to avoid this situation, in the design of TSP the minimum distance between A_1 and A_2 sliders are limited by mechanical stops, so a_1 never equals to a_2. When the distance between A_1 and A_2 is minimum, although the mechanism reaches the workspace boundary as well, it can still bear the payload in x direction, this situation is shown in Fig. 5a.
When

$$2l_1 = a_1 + a_2,$$

or

$$sin\theta(a_3 - \frac{a_1 + a_2}{2}) = cos\theta \sqrt{l_1^2 - (\frac{a_1 - a_2}{2})^2},$$

i.e. $M_1 = 0$ occurs, the mechanism will be in the forward kinematics singularity. For the former case, A_1, A_2, P are in-line and z_P equals 0. In this configuration, the velocity vector of pivot P is not able to be decided when A_1 and A_2 are given some velocities input. This singularity can also be avoid by restricting the minimum height of pivot P mechanically, for example, adopting mechanical limits to prevent P from reaching x-axis. For the latter case, points P, T, A_3 locate in-line, shown in Fig. 5b. In this configuration, links are not able to support moving platform to withstand the force perpendicular to PT and the mechanism can move T into the undesired position T_1. To solve the issues caused by this singularity, a constant angular offset α is added on the moving platform PQT. By selecting proper angle, the range of φ can be adjusted to avoid point T from approaching singularity.

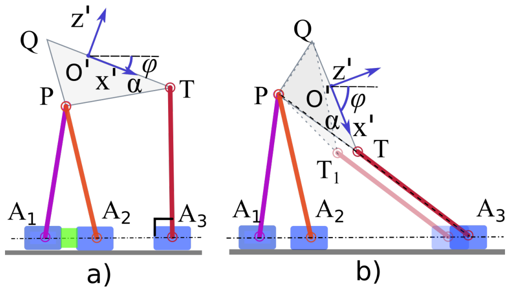

Figure 5: Typical singularity configurations of TSP. a) Mechanical stop is used to solve the inverse kinematics singularity caused by $a_1 = a_2$. b) Forward kinematics singularity pose formed by PTA$_3$ moving to in-line positions.

.

For parallel mechanisms, usually the position and orientation of the moving platform are coupled, thus the workspace of parallel mechanism are often given for a specified orientation. Table 2 lists the geometric parameters of links and PQT that fulfil the requirements of Table 1. Figure 6 shows the constant orientation workspaces of PRR mechanism of the TSP based on these parameters.

Table 2: Structure Parameters

configuration	pedal	treadmill
length of link 1 and link 2, $l_{1,2}$	$0.30m$	
length of link 3, l_3	$0.42m$	$0.45m$
length of TP, l_4	$0.09m$	$0.60m$
length of QT, l_5	$0.12m$	$0m$
angular offset, α	$33°$	$0°$
minimum distance between sliders	$0.1m$	
motion range of sliders in x direction	$0.08 — 1.12m$	

5 CONCLUSION

In this paper, we presented the kinematic design of a configurable terrain simulator platform. By reviewing the structure features and characteristic motions of robotic legs, we proposed the design specification of the TSP based on the leg of a hydraulically actuated quadruped robot. According to the desired specification, the motion mechanism of the TSP is designed based on a planar PRR parallel mechanism. Then the inverse kinematics and forward kinematics of this parallel mechanism are derived and the closed-form solutions for the forward and inverse kinematics are given. Furthermore the singularity features of this mechanism is fully researched based on the analysis of the

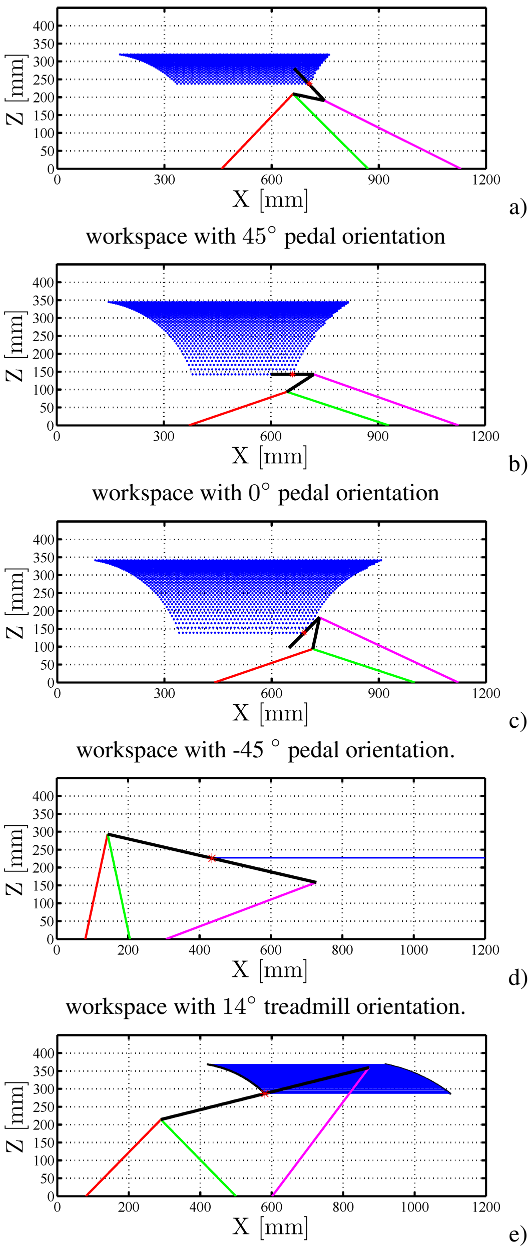

workspace with 45° pedal orientation

workspace with 0° pedal orientation

workspace with -45 ° pedal orientation.

workspace with 14° treadmill orientation.

workspace with -14 ° treadmill orientation.

Figure 6: Constant orientation workspace of the TSP mechanism.

Jacobian matrix. For different types of singularities, the corresponding impacts on motion were researched. Moreover, measures taken in the design are provided to solve the singularity problem. At last, based on properly selected parameters, the workspaces with different orientations and configurations of the TSP are obtained and presented.

6 ACKNOWLEDGEMENT

This research was funded by the Fondazione Istituto Italiano di Tecnologia. The authors would like to thank also the other members of the Dynamic Legged Systems Lab who contributed to the research presented in this paper.

REFERENCES

[1] J. T. Machado and M. F. Silva, "An overview of legged robots," in *International Symposium on Mathematical Methods in Engineering*, 2006.

[2] N. G. Tsagarakis, Z. Li, J. Saglia, and D. G. Caldwell, "The design of the lower body of the compliant humanoid robot ccub," in *Proceedings of IEEE International Conference on Robotics and Automation*, 2011, pp. 2035–2040.

[3] C. Semini, V. Barasuol, J. Goldsmith, M. Frigerio, M. Focchi, Y. Gao, and D. G. Caldwell, "Design of the hydraulically actuated, torque-controlled quadruped robot hyq2max," *IEEE/ASME Transactions on Mechatronics*, vol. 22, no. 2, pp. 635–646, April 2017.

[4] M. Raibert, K. Blankespoor, G. Nelson, R. Playter, and T. B. Team, "Bigdog, the rough-terrain quadruped robot," in *Proceedings of the 17th world congress*, vol. 17, no. 1. Proceedings Seoul, Korea, 2008, pp. 10 822–10 825.

[5] M. Hutter, C. Gehring, M. Bloesch, M. A. Hoepflinger, C. D. Remy, and R. Siegwart, "StarlETH: A compliant quadrupedal robot for fast, efficient, and versatile locomotion," in *15th International Conference on Climbing and Walking Robot-CLAWAR 2012*, 2012.

[6] K. J. Waldron, V. J. Vohnout, A. Pery, and R. B. McGhee, "Configuration design of the adaptive suspension vehicle," *The International Journal of Robotics Research*, vol. 3, no. 2, pp. 37–48, 1984.

[7] U. Saranli, M. Buehler, and D. E. Koditschek, "Rhex: A simple and highly mobile hexapod robot," *The International Journal of Robotics Research*, vol. 20, no. 7, pp. 616–631, 2001.

[8] M. H. Raibert, *Legged Robots That Balance*. The MIT Press, 1986.

[9] X. Liu, A. Rossi, and I. Poulakakis, "Spear: A monopedal robot with switchable parallel elastic actuation," in *2015 IEEE/RSJ International Conference on Intelligent Robots and Systems (IROS)*, Sept 2015, pp. 5142–5147.

[10] P. A. Willems and T. P. Gosseye, "Does an instrumented treadmill correctly measure the ground reaction forces?" *Biology Open*, vol. 2, no. 12, pp. 1421–1424, 2013.

[11] S. Hirose, Y. Fukuda, K. Yoneda, A. Nagakubo, H. Tsukagoshi, K. Arikawa, G. Endo, T. Doi, and R. Hodoshima, "Quadruped walking robots at tokyo institute of technology," *IEEE Robotics Automation Magazine*, vol. 16, no. 2, pp. 104–114, June 2009.

[12] C. Semini, N. G. Tsagarakis, E. Guglielmino, M. Focchi, F. Cannella, and D. G. Caldwell, "Design of HyQ - a hydraulically and electrically actuated quadruped robot," *IMechE Part I: Journal of Systems and Control Engineering*, vol. 225, no. 6, pp. 831–849, 2011.

[13] X. Rong, Y. Li, J. Ruan, and B. Li, "Design and simulation for a hydraulic actuated quadruped robot," *Journal of mechanical science and technology*, vol. 26, no. 4, pp. 1171–1177, 2012.

[14] C. M. Gosselin, S. Lemieux, and J. P. Merlet, "A new architecture of planar three-degree-of-freedom parallel manipulator," in *Proceedings of IEEE International Conference on Robotics and Automation*, vol. 4, Apr 1996, pp. 3738–3743 vol.4.

[15] P. Wenger and D. Chablat, "Workspace and Assembly modes in Fully-Parallel Manipulators : A Descriptive Study," in *ARK*. Austria: Kluwer Academic Publishers, 1998, pp. 117–126.

[16] M. Zein, P. Wenger, and D. Chablat, "Non-singular assembly-mode changing motions for 3-rpr parallel manipulators," *Mechanism and Machine Theory*, vol. 43, no. 4, pp. 480 – 490, 2008.